

12  
SC

LEVEL

AFGL-TR-79-0143

GLOBAL FREQUENCY DISTRIBUTION OF  
EXOSPHERIC TEMPERATURE

Jack W. Slowey

Smithsonian Institution  
Astrophysical Observatory  
60 Garden Street  
Cambridge, Massachusetts 02138

Scientific Report No. 1

Approved for public release; distribution unlimited

AD A 077293

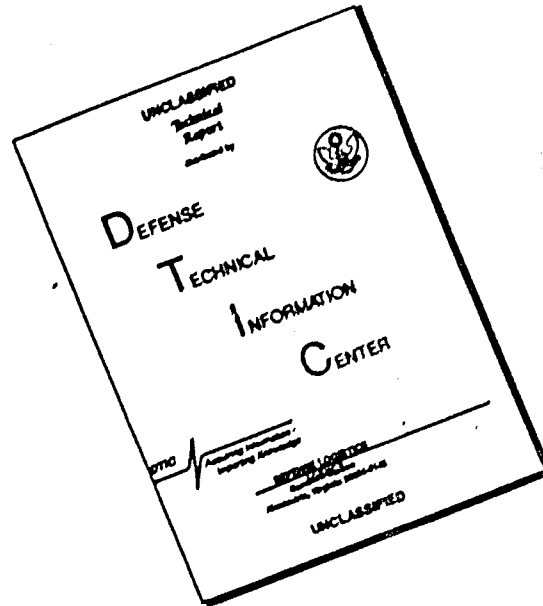
DDC  
RECEIVED  
NOV 27 1979  
A

DDC FILE COPY

AIR FORCE GEOPHYSICS LABORATORY  
AIR FORCE SYSTEMS COMMAND  
UNITED STATES AIR FORCE  
HANSCOM AFB, MASSACHUSETTS 01731

79 11 26 145

# DISCLAIMER NOTICE



THIS DOCUMENT IS BEST QUALITY AVAILABLE. THE COPY FURNISHED TO DTIC CONTAINED A SIGNIFICANT NUMBER OF PAGES WHICH DO NOT REPRODUCE LEGIBLY.

Qualified requestors may obtain additional copies from the Defense Documentation Center. All others should apply to the National Technical Information Service.

19 REPORT DOCUMENTATION PAGE		READ INSTRUCTIONS BEFORE COMPLETING FORM	
1. REPORT NUMBER 18 AFGL-TR-79-0143	2. GOVT ACCESSION NO.	3. RECIPIENT'S CATALOG NUMBER	
4. TITLE (and Subtitle) 6 GLOBAL FREQUENCY DISTRIBUTION OF EXOSPHERIC TEMPERATURE		5. TYPE OF REPORT & PERIOD COVERED Scientific Report No. 1	
7. AUTHOR(s) 10 Jack W. Slowey	15	6. PERFORMING ORG. REPORT NUMBER	
9. PERFORMING ORGANIZATION NAME AND ADDRESS Smithsonian Institution Astrophysical Observatory 60 Garden Street, Cambridge, Mass. 02138		8. CONTRACT OR GRANT NUMBER(s) F19628-78-C-0126 10a	
11. CONTROLLING OFFICE NAME AND ADDRESS Air Force Geophysics Laboratory Hanscom AFB, Massachusetts 01731 Monitor/Dorothy F. Gillette/LKB	16	10. PROGRAM ELEMENT, PROJECT, TASK AREA & WORK UNIT NUMBERS 6210JF 1247 669007AE	
14. MONITORING AGENCY NAME & ADDRESS (if different from Controlling Office) 10 25	11	12. REPORT DATE 5 July 1979	
		13. NUMBER OF PAGES	
		15. SECURITY CLASS. (of this report) Unclassified	
		15a. DECLASSIFICATION/DOWNGRADING SCHEDULE	
16. DISTRIBUTION STATEMENT (of this Report) Approved for public release; distribution unlimited. 14 SCIENTIFIC-1			
17. DISTRIBUTION STATEMENT (of the abstract entered in Block 20, if different from Report)			
18. SUPPLEMENTARY NOTES			
19. KEY WORDS (Continue on reverse side if necessary and identify by block number) Exospheric Temperature Atmospheric Models Thermosphere and Exosphere Atmospheric Variations			
20. ABSTRACT (Continue on reverse side if necessary and identify by block number) The distribution of exospheric temperature under all conditions of solar and geomagnetic activity and of spatial location was determined for two different models of the earth's thermosphere and exosphere. The two models were the 1971 Jacchia model and the U.S. Standard Atmosphere Supplements, 1966. Data from the past 12 solar cycles were used to determine the contribution of solar activity to the distributions. The contribution of geomagnetic activity was based on the distribution of geomagnetic activity for solar → next page			

044 850

LB

cycle 20. The spatial contribution was determined by analysis of the diurnal variation in exospheric temperature as given by the particular model. The resulting distributions indicate a mean exospheric temperature of approximately 900 K for either model.

Accession For	
NTIS Grant	<input checked="" type="checkbox"/>
DOC TAB	<input type="checkbox"/>
Unannounced	<input type="checkbox"/>
Justification	
By _____	
Distribution/	
Availability Codes	
Dist.	Avail and/or special
A	

# GLOBAL FREQUENCY DISTRIBUTION OF EXOSPHERIC TEMPERATURE

Jack W. Slowey

## INTRODUCTION

It was desired to determine the distribution of exospheric temperature as given by certain models of the earth's upper atmosphere. The required distributions were to cover all conditions of solar and geomagnetic activity as well as spatial location above the earth. They were to be employed to facilitate the use of the models in general-perturbation orbit integration. The models of interest were the 1971 Jacchia model (Jacchia, 1971) and the model given for heights above 120 km in the U.S. Standard Atmosphere Supplements, 1966 (COESA, 1966). For convenience, these models will be referred to as J71 and US66, respectively.

The problem was approached in three stages. In the first, the historical record of solar activity over the past 12 solar cycles was used to establish the effect of solar activity on the desired distributions. In the second, the effect of the diurnal temperature variations as given by the models was imposed. Finally, the distribution of geomagnetic disturbance was estimated, and its effect on the exospheric temperatures, as given by the models, was taken into account. These three stages of the investigation and the results from each are described in the following sections.

## SOLAR-ACTIVITY VARIATION

The earth's upper atmosphere undergoes a large variation in temperature and density in the course of the 11-year cycle of solar activity. The range of this variation is not, however, constant from one cycle to the next but

varies in accordance with the level of solar activity at maximum, a highly variable quantity. Thus, it is necessary to take a large portion of the historical record of solar activity into account in order to determine the statistical effect on the distribution of atmospheric temperature.

The historical record of sunspot numbers goes back to 1749. However, in most models of the thermosphere and exosphere, including those under consideration here, the variations associated with solar activity are correlated with the 10.7-cm radio flux from the sun. The record of the 10.7-cm solar flux goes back only to 1947 and is inadequate for the present purpose. It is necessary, therefore, to be able to relate the observed sunspot numbers to the corresponding 10.7-cm flux for use in the atmospheric models. The relation that was used was

$$\bar{F}_{10.7} = 49.4 + 0.97 \bar{R} + 17.6 \exp(-0.035 \bar{R}) \quad , \quad (1)$$

where  $\bar{F}_{10.7}$  is the mean adjusted 10.7-cm solar flux and  $\bar{R}$  is the mean Zurich sunspot number. This is a very slightly modified version of an equation previously developed by L. G. Jacchia and the author. It is reported (Euler, Lundquist and Vaughan, 1978) to give a correlation coefficient of 0.98 with a data base of  $\bar{F}_{10.7}$  from 67 to 260, where the means of  $F_{10.7}$  and of  $R$  were 13-month running means of the monthly mean values (the 13-month running mean is centered on the month in question and gives half weight to the months 6 months before and 6 months after that month).

The distribution of the nighttime minimum in the exospheric temperature was obtained by sampling every third monthly value of the 13-month running means of the sunspot number. Smoothing over 6-month intervals is usually recommended in connection with the atmospheric models. The 13-month means — which are routinely used in solar activity prediction — were already available, however, and it was clear that the slightly greater smoothing would have very little effect on the resulting distribution. Equation (1) was used to obtain the mean 10.7-cm flux, which was then converted to temperature by

Table 1. Distribution of global minimum exospheric temperature as computed from the J71 and US66 atmospheric models.

Temp. Interval* (°K)	J71 Model			US66 Model		
	N <sup>†</sup>	N/N <sub>T</sub> (%)	f(K <sup>-1</sup> )	N	N/N <sub>T</sub> (%)	f(K <sup>-1</sup> )
0 - + 10	64	12.0	1.20 × 10 <sup>-2</sup>	61	11.5	1.15 × 10 <sup>-2</sup>
+ 10 - + 20	45	8.5	0.85	41	7.7	0.77
+ 20 - + 30	34	6.4	0.64	32	6.0	0.60
+ 30 - + 40	24	4.5	0.45	23	4.3	0.43
+ 40 - + 60	34	6.4	0.32	33	6.2	0.31
+ 60 - + 80	27	5.1	0.25	29	5.5	0.27
+ 80 - +100	39	7.3	0.37	32	6.0	0.30
+100 - +120	36	6.8	0.34	33	6.2	0.31
+120 - +140	32	6.0	0.30	29	5.5	0.27
+140 - +160	29	5.5	0.27	24	4.5	0.23
+160 - +180	22	4.1	0.21	30	5.6	0.28
+180 - +200	23	4.3	0.22	19	3.6	0.18
+200 - +230	23	4.3	0.14	26	4.9	0.16
+230 - +260	19	3.6	0.12	27	5.1	0.17
+260 - +300	22	4.1	0.10	19	3.6	0.09
+300 - +350	23	4.3	0.09	26	4.9	0.10
+350 - +400	13	2.4	0.05	15	2.8	0.06
+400 - +450	8	1.5	0.03	12	2.3	0.045
+450 - +550	12	2.3	0.023	13	2.4	0.024
+550 - +650	3	0.6	0.006	6	1.1	0.011
+650 - +750	0	0.0	0.000	2	0.4	0.004

\* Relative to the temperature corresponding to  $\bar{R} = 0$  ( $\bar{F}_{10.7} = 67$ ). This temperature is 596.1 K for the J77 model and 603.2 K for the US66 model.

† N is the number of data points in the interval, N<sub>T</sub> is the total number of data points (= 532).



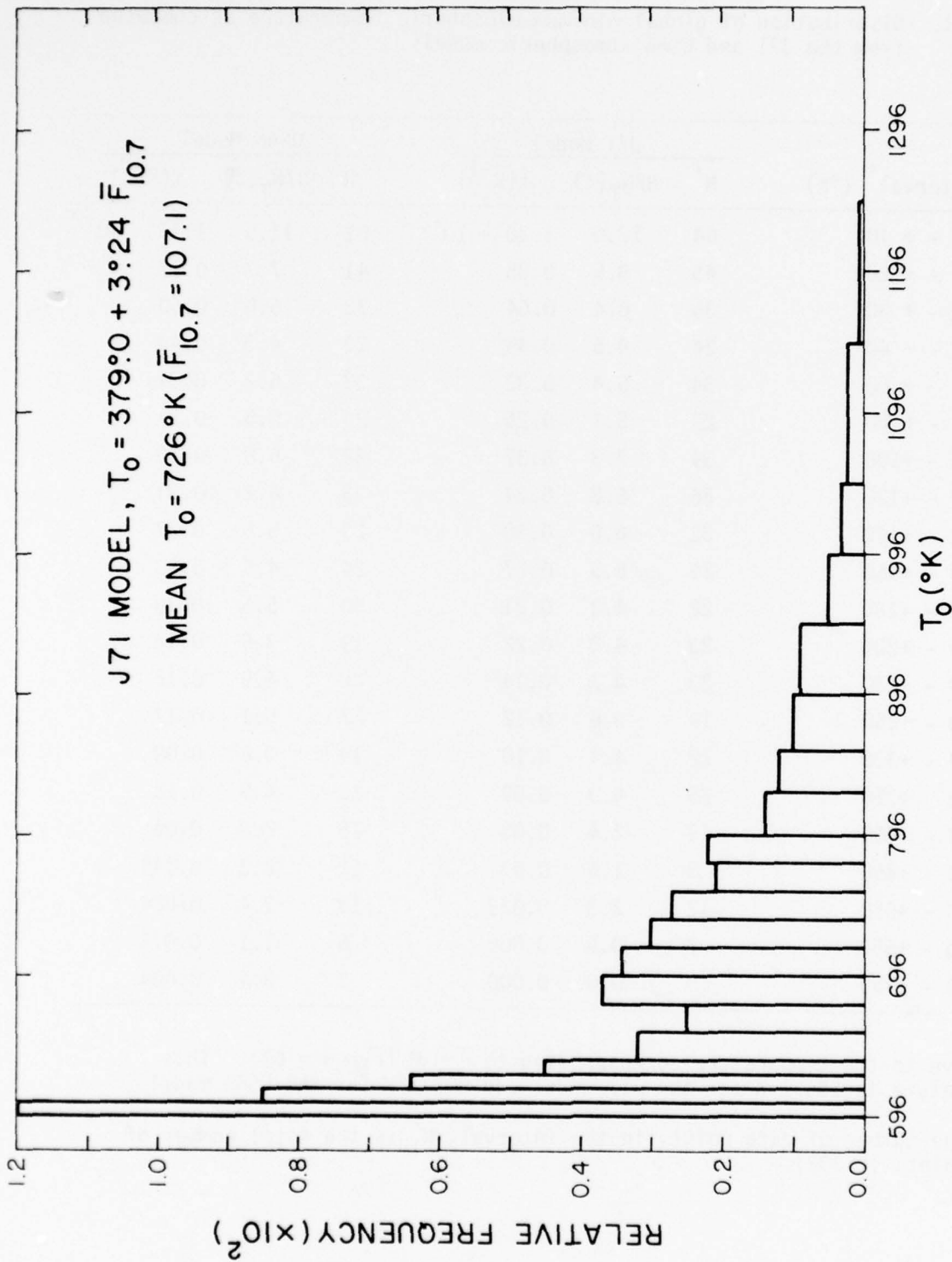


Figure 1a. Distribution of global minimum exospheric temperature over 12+ solar cycles, J71 model.

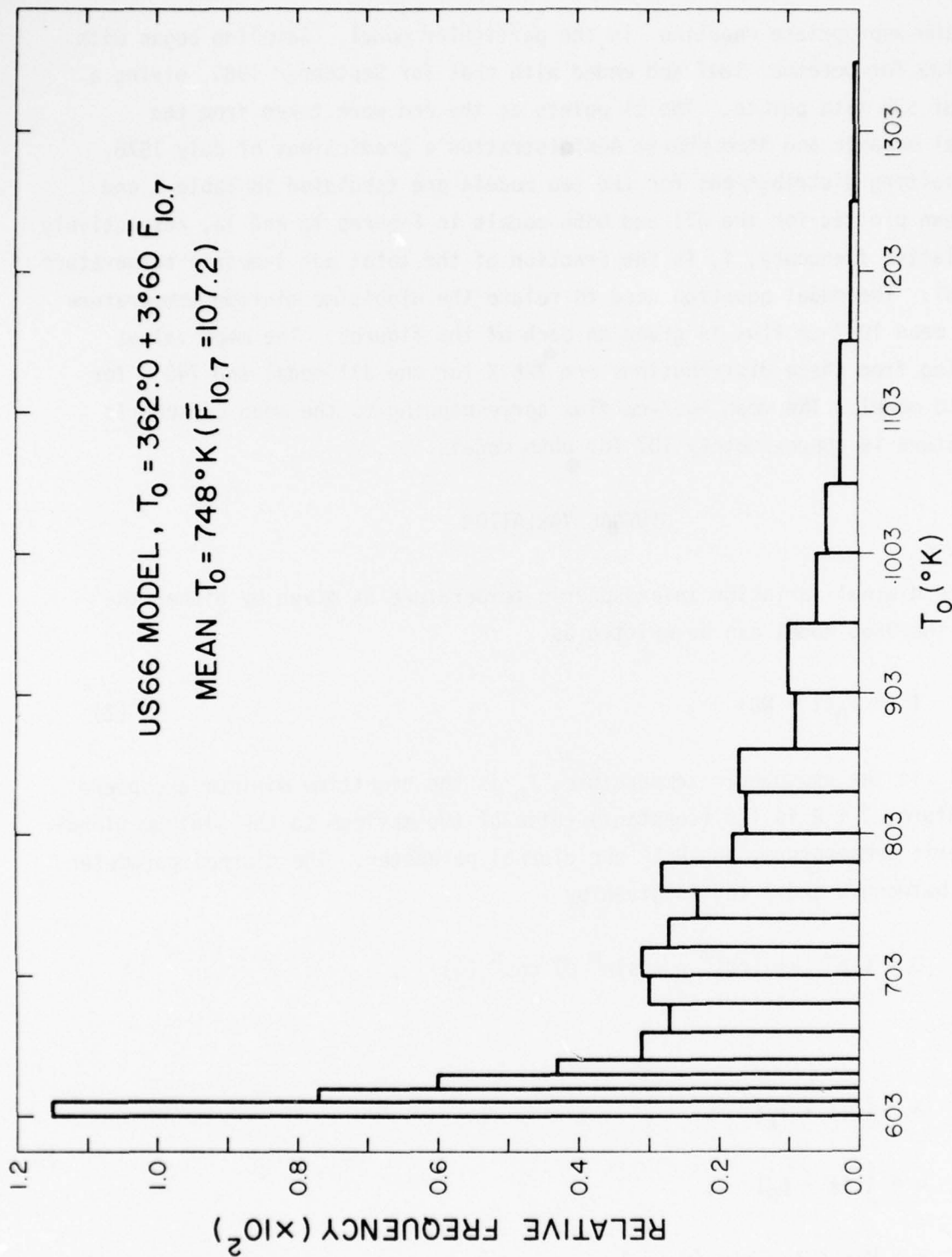


Figure 1b. Distribution of global minimum exospheric temperature over 12+ solar cycles, US66 model.

using the appropriate equation in the particular model. Sampling began with the value for December 1847 and ended with that for September 1980, giving a total of 532 data points. The 11 points at the end were taken from the National Oceanic and Atmospheric Administration's predictions of July 1978. The resulting distributions for the two models are tabulated in Table 1 and are shown plotted for the J71 and US66 models in Figures 1a and 1b, respectively. The relative frequency,  $f$ , is the fraction of the total per 1-degree temperature interval. The model equation used to relate the nighttime minimum temperature to the mean 10.7-cm flux is given on each of the figures. The mean values resulting from these distributions are 726 K for the J71 model and 748 K for the US66 model. The mean 10.7-cm flux corresponding to the mean exospheric temperature is approximately 107 for both models.

#### DIURNAL VARIATION

The diurnal variation in exospheric temperature as given by either the J71 or the US66 model can be written as

$$T_{\infty} = T_0(1 + RD) \quad , \quad (2)$$

where  $T_{\infty}$  is the exospheric temperature,  $T_0$  is the nighttime minimum exosphere temperature,  $1 + R$  is the (constant) ratio of the maximum to the minimum global exospheric temperature, and  $D$  is the diurnal parameter. The diurnal parameter varies between 0 and 1 and is given by

$$D = \sin^m \theta + (\cos^m \eta - \sin^m \theta) \cos^n \left( \frac{\tau}{2} \right) \quad ,$$

with

$$\theta = \frac{1}{2} |\phi + \phi_B| \quad ,$$

$$\eta = \frac{1}{2} |\phi - \phi_B| \quad ,$$

$$\tau = H + \beta + p \sin (H + \gamma) \quad , \quad (3)$$

where  $\phi$  is the latitude of the point in question,  $\phi_B$  is the latitude of the maximum in exospheric temperature, and  $H$  is the hour angle of the sun. In the case of the J71 model,  $\phi_B$  is set equal to the declination of the sun, while in the US66 model,  $\phi_B = 0$ . Constants for the two models are

$$R = 0.3 \quad , \quad m = 2.2 \quad , \quad n = 3.0 \quad , \quad \beta = -37^\circ \quad , \quad p = 6^\circ \quad , \quad \gamma = 43^\circ$$

and

$$R = 0.28 \quad , \quad m = 1.5 \quad , \quad n = 2.5 \quad , \quad \beta = -45^\circ \quad , \quad p = 12^\circ \quad , \quad \gamma = 45^\circ$$

for the J71 and US66 models, respectively.

A computer program was written to integrate numerically the area on the globe between the point of minimum exospheric temperature and the exospheric isotherm defined by a particular value of the diurnal parameter. Results from this program are tabulated for both models in Table 2 and are plotted in Figure 2a. Table 2 gives results for the two extreme cases of equinox and solstice in the case of the J71 model. As can be seen, the differences between the results for the two cases are quite small. Thus, the results for the single case of equinox were taken to represent the distribution for any time of the year in the subsequent computations with the J71 model.

The diurnal distribution of exospheric temperature is quite different in the two atmospheric models as a result of the differences in the model constants. This is evident from the isotherm plots included with the published models. It can also be seen in Figure 2b, where the diurnal temperature distribution — which depends on the slope of the diurnal area curve in Figure 2a — is plotted for each of the two models for the case where the minimum exospheric temperatures are equal to the mean values given above. In the J71 model, the frequency is much larger near minimum temperature than it is at higher temperature because the isotherms are much more widely spaced near minimum temperature than they are for higher temperatures. In the US66 model, the variation in spacing is much less, and the isotherms are actually closer together at minimum than they are at maximum.

Table 2. Integrated global isotherm areas as a function of the diurnal temperature parameter, D, for the J71 and US66 atmospheric models (total area = 1).

D	J71 Model		US66 Model
	$\phi_B = 0^\circ 0$	$\phi_B = 23^\circ 5$	$\phi_B = 0^\circ 0$
0.00	0.0000	0.0000	0.0000
0.05	0.1037	0.1014	0.0397
0.10	0.1787	0.1748	0.0841
0.15	0.2452	0.2398	0.1307
0.20	0.3063	0.2995	0.1791
0.25	0.3635	0.3551	0.2287
0.30	0.4174	0.4074	0.2794
0.35	0.4685	0.4576	0.3310
0.40	0.5158	0.5061	0.3831
0.45	0.5625	0.5533	0.4357
0.50	0.6055	0.5991	0.4886
0.55	0.6473	0.6437	0.5414
0.60	0.6883	0.6870	0.5938
0.65	0.7286	0.7290	0.6454
0.70	0.7685	0.7694	0.6965
0.75	0.8078	0.8090	0.7475
0.80	0.8469	0.8481	0.7983
0.85	0.8855	0.8866	0.8490
0.90	0.9239	0.9248	0.8996
0.95	0.9620	0.9626	0.9500
1.00	1.0000	1.0000	1.0000

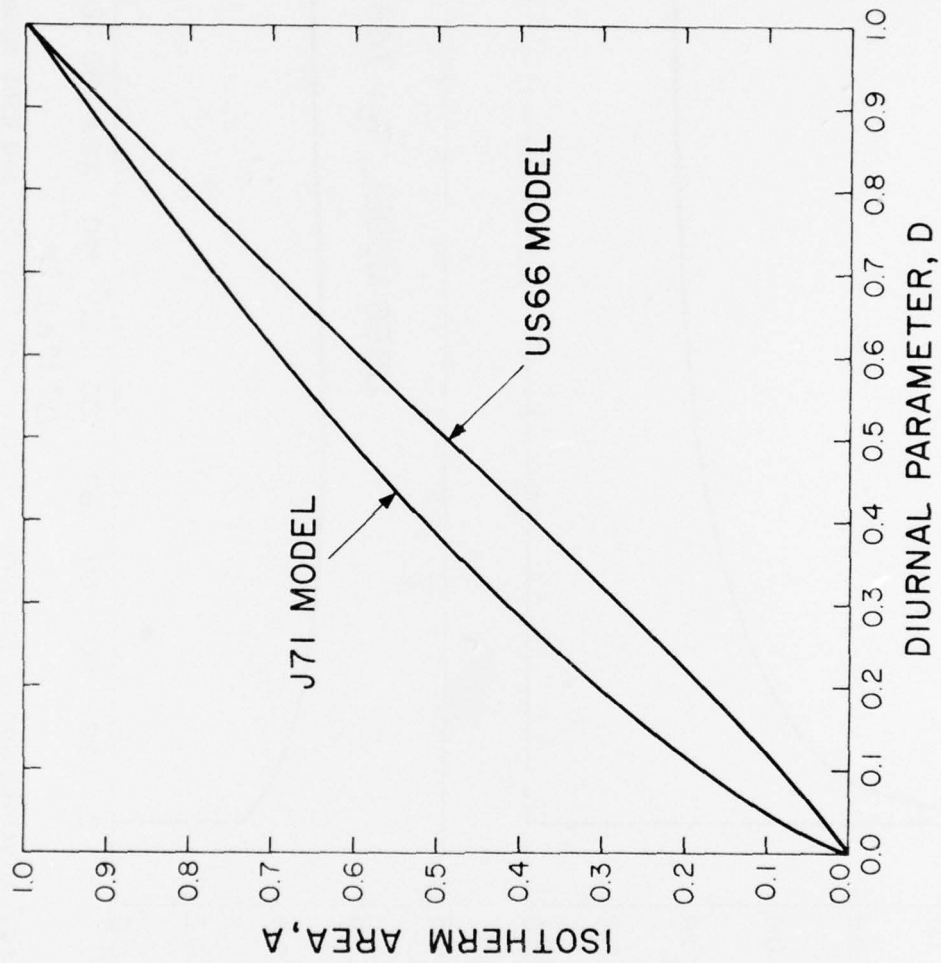


Figure 2a. Integrated global isotherm areas for J71 and US66 models.

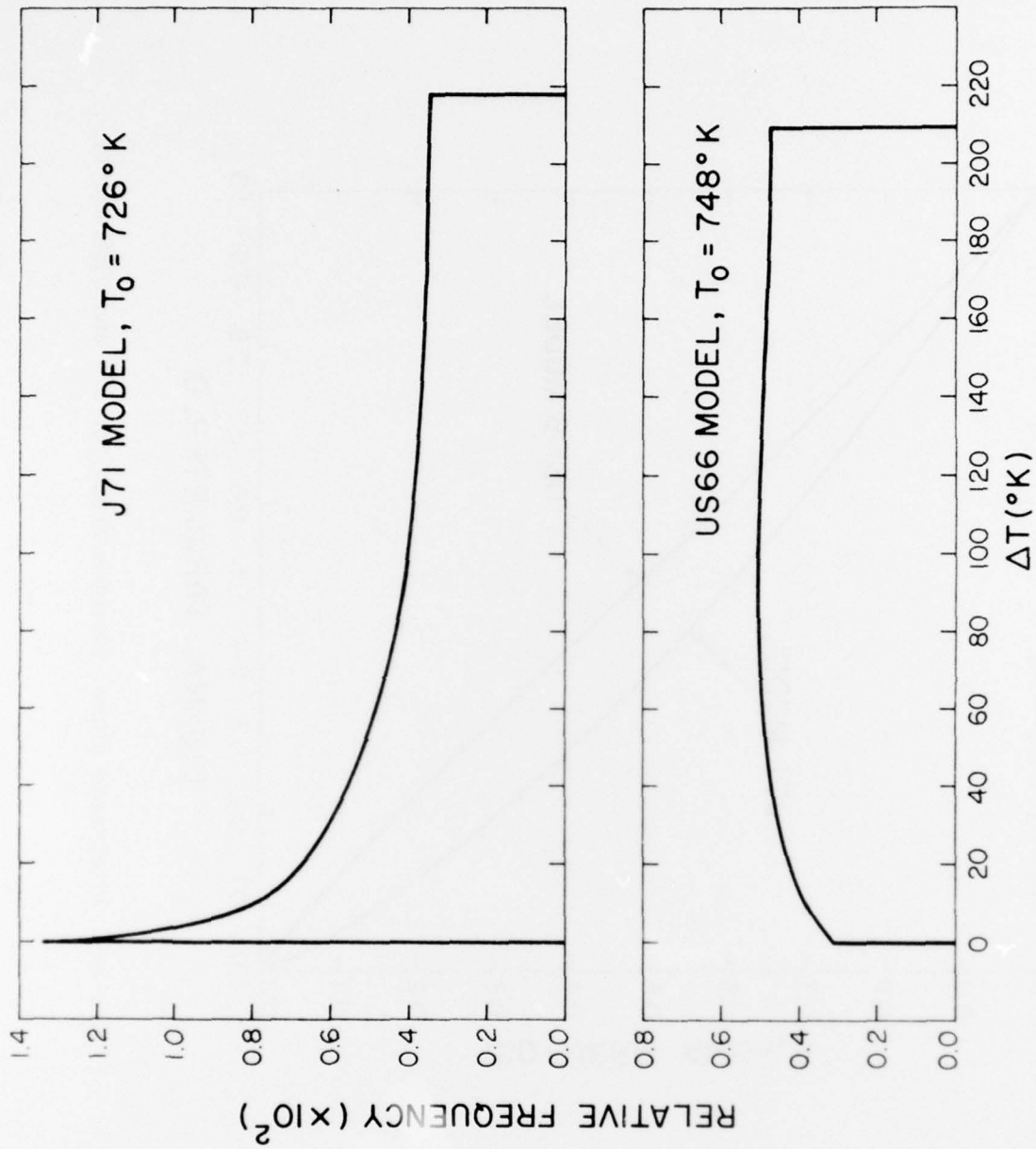


Figure 2b. Global distribution of exospheric temperature from J71 and US66 models computed for mean value of global minimum exospheric temperature.

The global distribution of exospheric temperature was calculated for the two models from the corresponding distribution of minimum temperature by computing

$$f_G(T_1, T_2) = \sum_{T_0} \frac{f_0(T_0) \Delta T_0 (A_2 - A_1)}{T_2 - T_1}, \quad (4)$$

where  $f_G(T_1, T_2)$  is the global relative frequency per degree in the interval between  $T_1$  and  $T_2$ ,  $f_0(T_0)$  is the relative frequency per degree of the minimum temperature  $T_0$ , and  $A_1$  and  $A_2$  are the global isotherm areas corresponding to the two diurnal parameters computed from

$$D_i = \frac{T_i - T_0}{T_0 R} \quad (5)$$

The sum was taken with steps of  $1^\circ$  in  $T_0$  and values of  $A$  were computed by interpolation from Table 2.

The resulting distributions ( $K_p = 0$ ) are given for both models in Table 3 and are plotted in Figure 3a for the J71 model and in Figure 3b for the US66 model. Mean values of the exospheric temperatures given by these distributions are 817 and 855°K, respectively, for the J71 and US66 models.

#### GEOMAGNETIC VARIATION

To determine the effect of the geomagnetic variation on the distributions, it was first necessary to obtain the distribution of geomagnetic disturbance. The historical record of the geomagnetic index commences in 1932 and, hence, encompasses the last 4 complete solar cycles (17-20). Only data beginning midway through cycle 19 were readily available to the author, however. Data from cycle 19 were excluded both because they represented only a partial cycle and might be biased for that reason and because cycle 19 itself was extremely



Table 3. Global distribution of exospheric temperature from the J71 and US66 atmospheric models for  $K_p = 0$ .

Temp. Interval* ( $^{\circ}\text{K}$ )	J71 Model		US66 Model	
	$N/N_T(\%)$	$f(^{\circ}\text{K}^{-1})$	$N/N_T(\%)$	$f(^{\circ}\text{K}^{-1})$
0 - +20	2.8	$0.141 \times 10^{-2}$	1.2	$0.061 \times 10^{-2}$
+20 - +40	4.6	0.229	2.7	0.134
+40 - +60	4.9	0.247	3.6	0.180
+60 - +80	5.1	0.254	4.3	0.217
+80 - +100	5.5	0.274	5.0	0.251
+100 - +120	6.0	0.298	5.6	0.282
+120 - +140	6.3	0.315	6.2	0.309
+140 - +160	6.6	0.328	6.7	0.333
+160 - +180	6.7	0.335	6.8	0.340
+180 - +200	6.1	0.303	5.6	0.281
+200 - +230	7.2	0.241	7.1	0.236
+230 - +260	6.2	0.205	6.5	0.215
+260 - +300	7.1	0.178	7.6	0.191
+300 - +350	7.1	0.141	7.8	0.155
+350 - +400	5.2	0.104	6.1	0.122
+400 - +450	3.8	0.075	4.6	0.092
+450 - +500	2.8	0.055	3.5	0.070
+500 - +550	2.1	0.041	2.6	0.052
+550 - +600	1.5	0.030	2.0	0.040
+600 - +700	1.6	0.016	2.4	0.024
+700 - +800	0.7	0.007	1.2	0.012
+800 - +900	0.3	0.003	0.6	0.006
+900 - +1000	0.1	0.001	0.2	0.002
+1000 - +1100	0.0	0.000	0.1	0.001
+1100 - +1200	0.0	0.000	0.0	0.000

\*Relative to  $596 \pm 1$  K for the J71 model and  $603 \pm 2$  K for the US66 model.

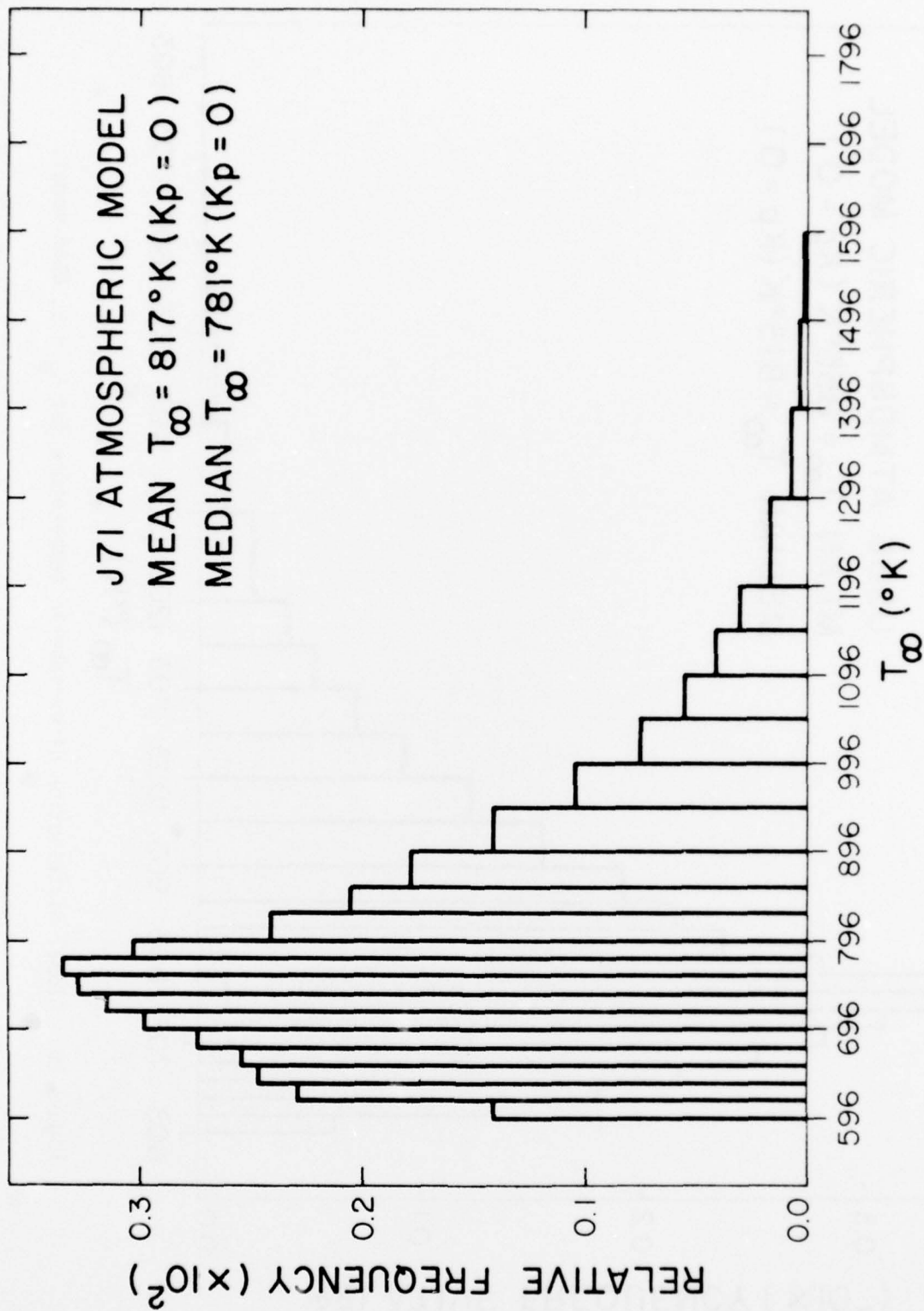


Figure 3a. Global distribution of exospheric temperature for  $K_p = 0$ , J71 model.

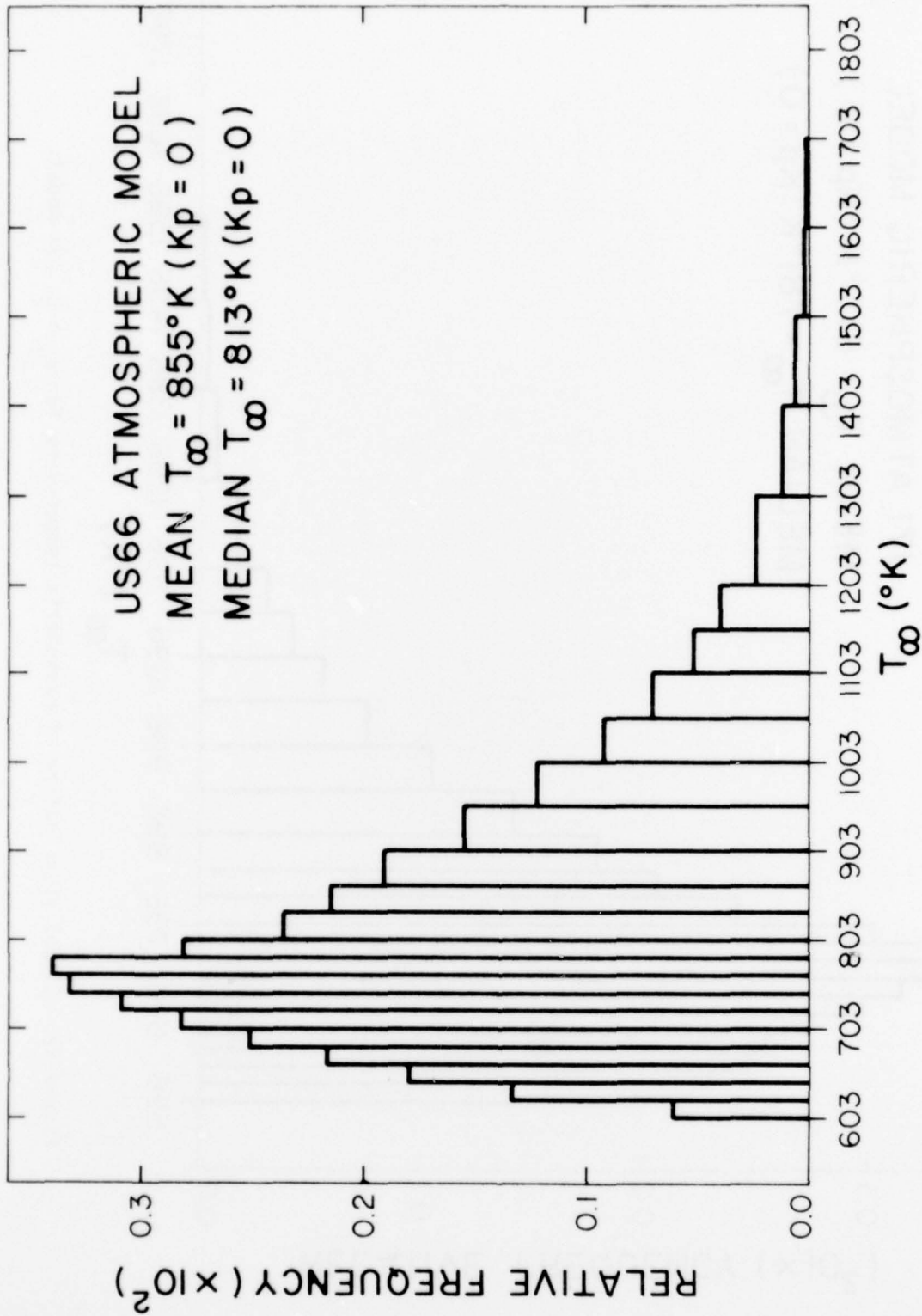


Figure 3b. Global distribution of exospheric temperature for  $K_p = 0$ , US66 model.

Table 4. Distribution of the  $K_p$  geomagnetic index over the most recent solar cycle.

$K_p$	$\Delta T_G^*$ ( $^{\circ}K$ )	N	$f = N/N_T$	$\Sigma f$
0	0.0	130	.0448	.0448
0+	9.3	254	.0632	.1080
1-	18.8	286	.0712	.1792
1	28.1	309	.0769	.2561
1+	37.4	315	.0784	.3345
2-	46.9	351	.0874	.4219
2	56.2	333	.0829	.5047
2+	65.6	304	.0757	.5804
3-	75.2	316	.0786	.6590
3	84.6	333	.0829	.7419
3+	94.1	260	.0647	.8066
4-	103.9	207	.0515	.8581
4	113.6	157	.0391	.8972
4+	123.5	127	.0316	.9288
5-	134.0	93	.0231	.9520
5	144.4	61	.0152	.9671
5+	155.4	41	.0102	.9774
6-	167.5	29	.0072	.9846
6	180.1	23	.0057	.9903
6+	194.1	10	.0025	.9928
7-	210.4	9	.0022	.9950
7	228.9	5	.0012	.9963
7+	251.0	3	.0007	.9970
8-	279.0	4	.0010	.9980
8	313.4	4	.0010	.9990
8+	357.6	2	.0005	.9995
9-	417.5	1	.0002	.9998
9	495.1	1	.0002	1.0000

\*  $\Delta T_G = 28^{\circ} K_p + 0.03 \exp(K_p)$ .

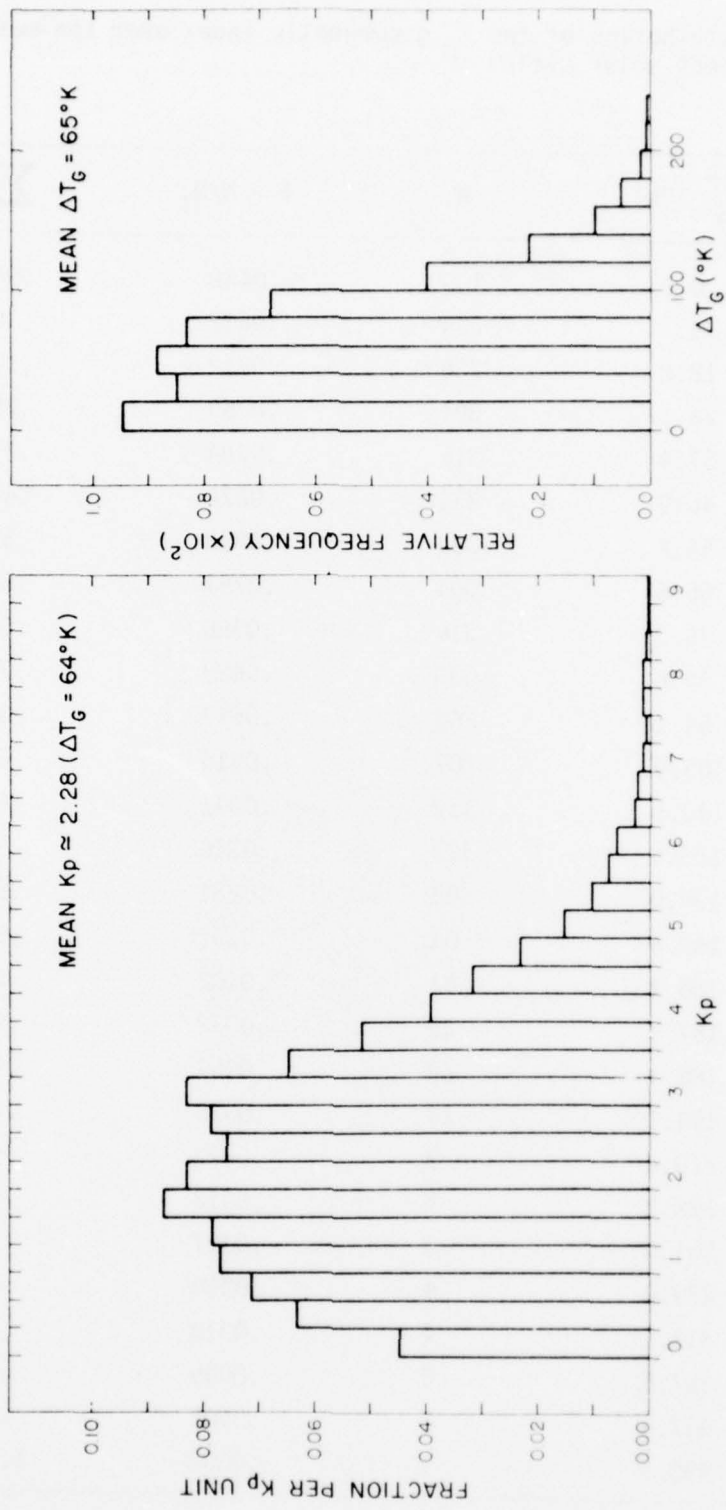


Figure 4. Distribution of 3-hourly  $K_p$  index over last 11-year solar cycle (1/8 sample) and resulting distribution of the increase in exospheric temperature (histogram at right) as given by relation used in J71 and US66 atmospheric models.

Table 5. Global frequency distribution of exospheric temperature from the J71 and US66 atmospheric models with the geomagnetic temperature variation included.

Temp. Interval* ( $^{\circ}\text{K}$ )	J71 Model		US66 Model	
	$N/N_T$ (%)	$F$ ( $^{\circ}\text{K}^{-1}$ )	$N$ (%)	$F$ ( $^{\circ}\text{K}^{-1}$ )
0 - +20	0.2	$0.010 \times 10^{-2}$	0.1	$0.004 \times 10^{-2}$
+20 - +40	0.8	0.040	0.4	0.020
+40 - +60	1.6	0.082	0.9	0.047
+60 - +80	2.5	0.127	1.6	0.081
+80 - +100	3.4	0.171	2.4	0.121
+100 - +120	4.2	0.211	3.3	0.163
+120 - +140	4.9	0.243	4.0	0.202
+140 - +160	5.4	0.268	4.8	0.238
+160 - +180	5.8	0.288	5.4	0.269
+180 - +200	6.0	0.301	5.8	0.289
+200 - +230	9.1	0.302	8.8	0.293
+230 - +260	8.5	0.282	8.3	0.278
+260 - +300	9.8	0.244	9.8	0.245
+300 - +350	9.8	0.196	10.2	0.204
+350 - +400	7.6	0.152	8.3	0.166
+400 - +450	5.8	0.116	6.6	0.132
+450 - +500	4.3	0.085	5.1	0.102
+500 - +550	3.2	0.063	3.9	0.078
+550 - +600	2.3	0.046	3.0	0.059
+600 - +700	2.8	0.028	3.7	0.037
+700 - +800	1.3	0.013	2.0	0.020
+800 - +900	0.6	0.006	1.0	0.010
+900 - +1000	0.2	0.002	0.5	0.005
+1000 - +1100	0.1	0.001	0.2	0.002
+1100 - +1200	0.0	0.000	0.1	0.001

\* Relative to  $596 \pm 1$  K for the J71 model and  $603 \pm 2$  K for the US66 model.

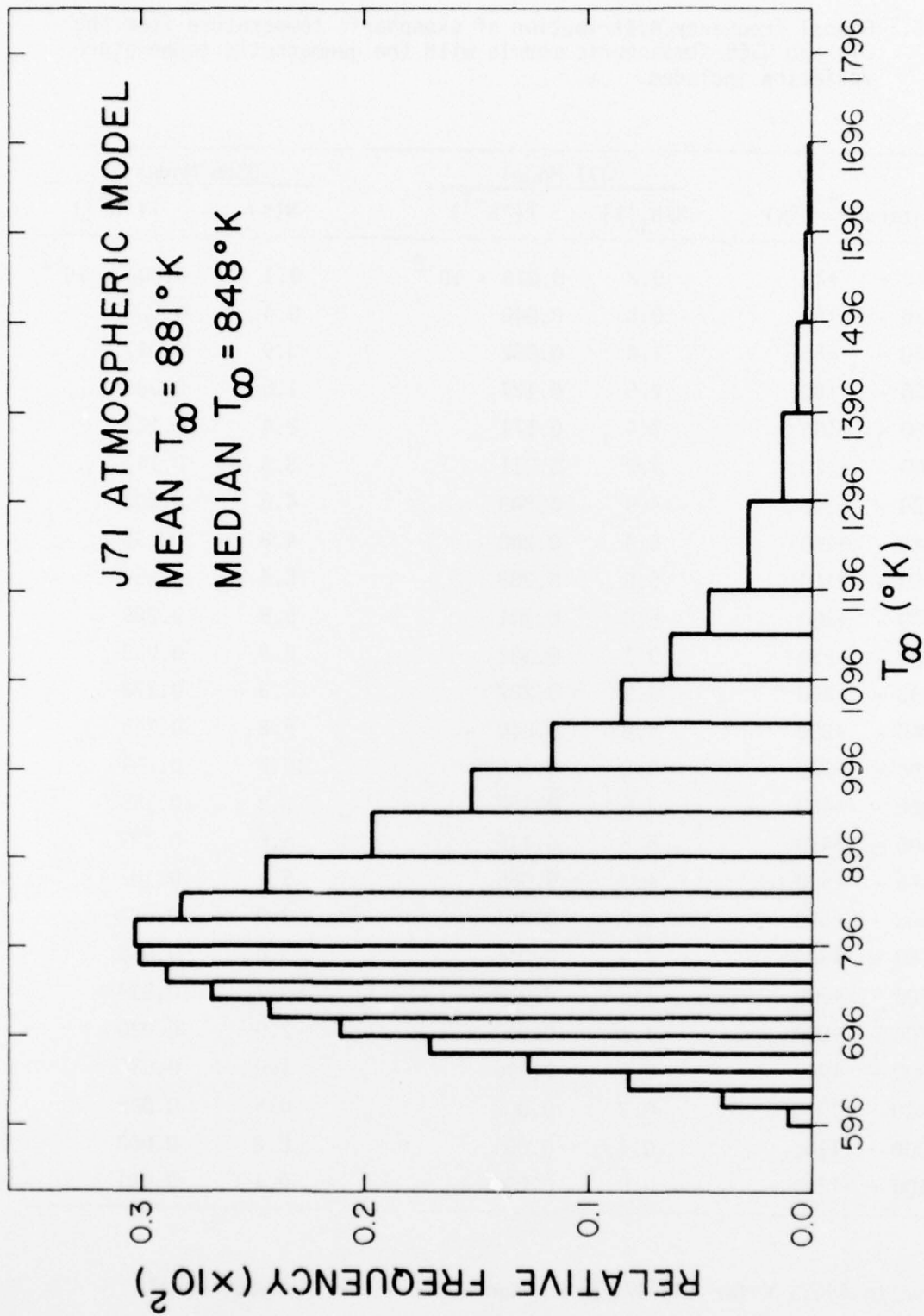


Figure 5a. Global distribution of exospheric temperature including geomagnetic variation, J71 model.

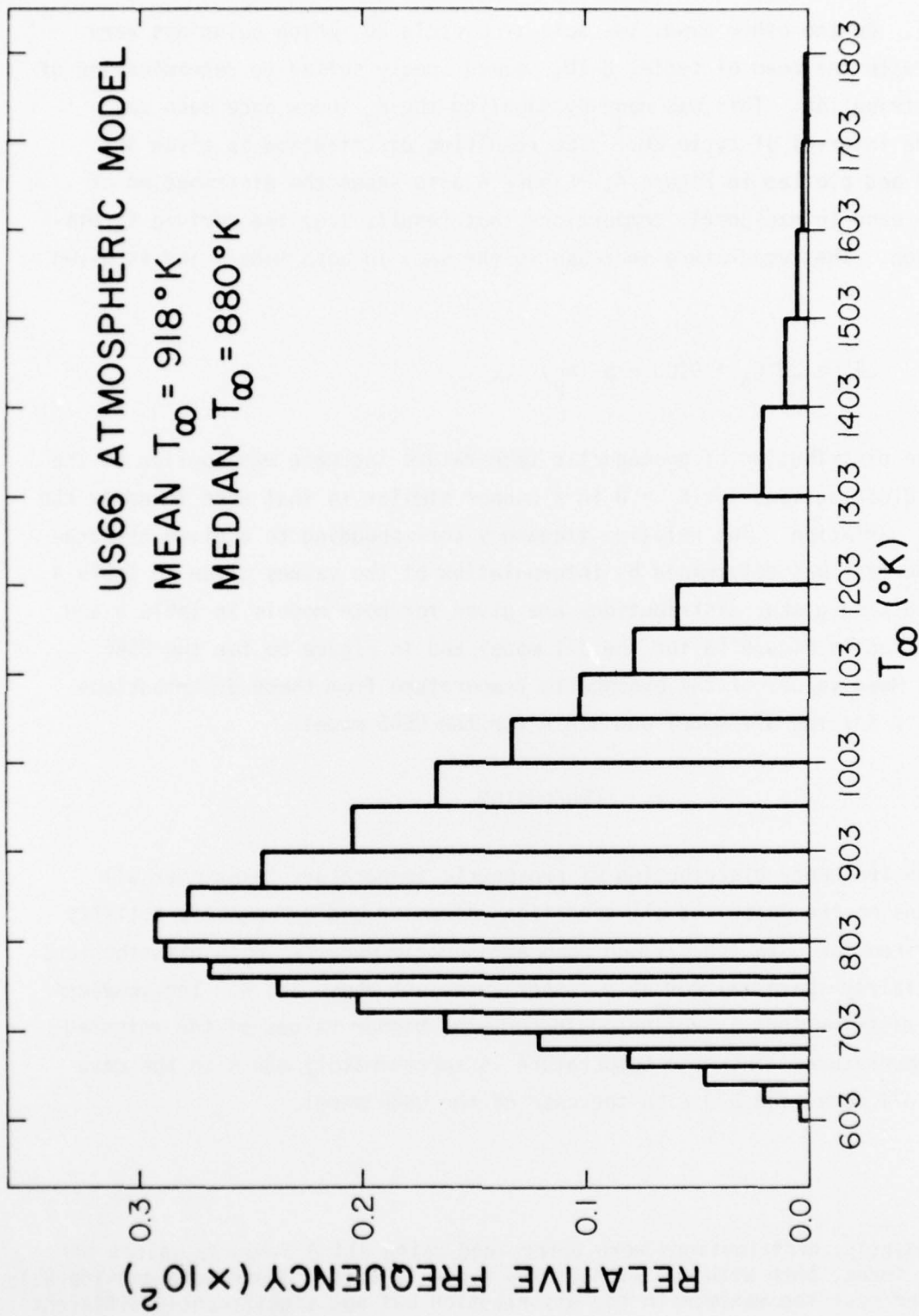


Figure 5b. Global distribution of exospheric temperature including geomagnetic variation, US66 model.



unusual. On the other hand, the data from cycle 20, which coincides very nearly with the mean of cycles 8-20, seemed ideally suited to determination of the distribution. This was done by sampling the  $K_p$  index once each day over the interval of cycle 20.\* The resulting distribution is given in Table 4 and plotted in Figure 4. Figure 4 also shows the distribution of the increase in exospheric temperature that results from the derived  $K_p$  distribution. The temperature increase is the same in both models and is given by

$$\Delta T_G = 28^\circ K_p + 0.03 \exp(K_p) .$$

The distribution of geomagnetic temperature increase was applied to the global distributions for  $K_p = 0$  in a manner similar to that used to apply the diurnal variation. The relative frequency corresponding to a given temperature increase was determined by interpolation of the values given in Table 4. The resulting global distributions are given for both models in Table 5 and are plotted in Figure 5a for the J71 model and in Figure 5b for the US66 model. Mean values of the exospheric temperature from these distributions are 881 K for the J71 model and 918 K for the US66 model.

#### CONCLUSION

The frequency distribution of exospheric temperature taken over all locations on the earth and all conditions of solar and geomagnetic activity was derived for both the J71 and US66 atmospheric models. Both distributions have a fairly sharp maximum at a temperature just above 800 K. The skewness of the distributions is reflected in somewhat higher values of the weighted mean temperature. The mean temperature is approximately 880 K in the case of the J71 model and 920 K in the case of the US66 model.

\* Subsequently, distributions were determined using all 8 3-hourly values of the  $K_p$  index, both with and without the cycle 19 data. These were considerably smoother near the maximum in the distribution but not significantly different in any other way.

#### REFERENCES

- COESA (U.S. Committee on the Extension of the Standard Atmosphere), 1966. U.S. Standard Atmosphere Supplements, 1966. U.S. Government Printing Office, Washington, D.C., 289 pp.
- Euler, H. C., Lundquist, C. A., and Vaughan, W. W., 1978. MSFC solar activity predictions for satellite orbital lifetime estimation. Paper presented to Solar-Terrestrial Predictions Workshop, Boulder, Colorado, 23-27 April, 1979.
- Jacchia, L. G., 1971. Revised static models of the thermosphere and exosphere with empirical temperature profiles. Smithsonian Astrophys. Obs. Spec. Rep. No. 332, 113 pp.